Stabilisation of the Arrival Time of a Relativistic Electron Beam to the 50 fs Level

J. Roberts,[1,2] P. Skowronski,[2] P.N. Burrows,[1] G.B. Christian,[1] R. Corsini,[2] A. Ghigo,[3] F. Marcellini,[3] and C. Perry[1]

[1] *John Adams Institute (JAI), University of Oxford, Denys Wilkinson Building, Keble Road, Oxford, OX1 3RH, United Kingdom*

[2] *The European Organization for Nuclear Research (CERN), Geneva 23, CH-1211, Switzerland*

[3] *Laboratori Nazionali di Frascati (LNFN), Via Enrico Fermi, 40, 00044 Frascati RM, Italy*

(Dated: May 29, 2017)

We report the results of a low-latency beam phase feed-forward system built to stabilise the arrival time of a relativistic electron beam. The system was operated at the Compact Linear Collider (CLIC) Test Facility (CTF3) at CERN where the beam arrival time was stabilised to approx. 50 fs. The system latency was 350 ns and the correction bandwidth > 23 MHz. The system meets the requirements for CLIC and could have applications at future free-electron lasers.

High-energy linear electron-positron colliders have been proposed as next-generation particle accelerators for exploring the subatomic world with increased precision. They provide sensitivity to new physics processes, beyond those described by the Standard Model (SM) of elementary particle interactions, at mass scales that can exceed the reach of the CERN Large Hadron Collider (LHC) by more than an order of magnitude [1].

The Compact Linear Collider (CLIC) [2] is the most technologically mature concept of a high-energy lepton collider for enabling direct searches for new physics in the multi-TeV energy regime. It uses a novel two beam acceleration concept to achieve a high accelerating gradient of 100 MV/m and centre-of-mass collision energies of up to 3 TeV. This energy reach, combined with high-luminosity of the electron-positron collisions, will also enable precise measurements of properties of the Higgs boson [3] and the top quark, and provide sensitivity to beyond-SM phenomena at mass scales of up to 10-100 TeV [1].

The CLIC two-beam acceleration concept is shown schematically in Fig. 1. The 12 GHz RF power used to accelerate the main high energy electron and positron beams is generated by decelerating high intensity electron 'drive beams'. The power is extracted from the drive beams and transferred to the main beams in decelerator sectors; two drive beams with 25 decelerator sectors each are required for a 3 TeV collider. Prior to power extraction the drive beam comprises a 240 ns-long pulse of 2.4 GeV electrons bunched with a frequency of 12 GHz; the pulse repetition rate is 50 Hz.

A major challenge is the synchronisation of the arrival of the drive and main beams at the power-extraction and transfer structures to better than 50 fs rms. This requirement limits the luminosity loss, resulting from subsequent energy errors of the main beams, to less than 1% of the design value [4]. Free-electron lasers (FELs) also demand a high degree of beam arrival-time stability w.r.t. an externally-applied laser beam for the purpose of seeding of lasing by the electron beam. An RF phase and amplitude feedback utilising electro-optic beam arrival time monitors in this context was reported in [5].

We express the temporal stability of the drive beam in terms of phase stability at the 12 GHz acceleration frequency. An arrival time jitter of 50 fs rms is equivalent to a phase jitter of 0.2° at 12 GHz. In the CLIC design the incoming drive-beam phase jitter cannot be guaranteed to be better than 2° [2]. A mechanism to improve the phase stability by an order of magnitude is therefore required. The correction must be applied to the full drive beam pulse length and have a bandwidth exceeding 17.5 MHz [6].

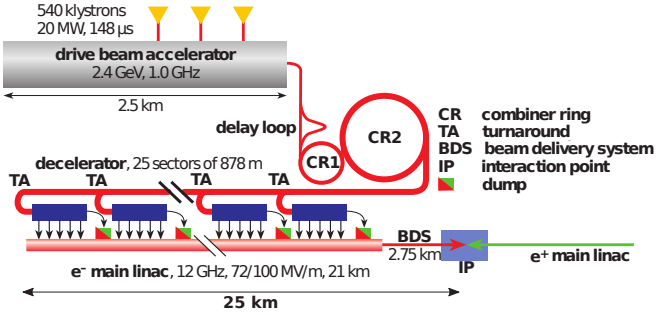

FIG. 1. Schematic of the CLIC drive-beam concept showing the electron acceleration complex [1].

This is implemented via a 'phase feed-forward' (PFF) system which measures the incoming beam phase and provides a correction to the same beam pulse after it has traversed the turnaround loop (TA in Fig. 1). One PFF system will be installed in each deceleration sector. The correction is provided by electromagnetic kickers in a 4-bend chicane: bunches arriving early (late) in time have their path through the chicane lengthened (shortened) respectively. A particular challenge is that the PFF latency must be shorter than the beam flight time of approx. 250 ns around the turnaround loop.

We describe a prototype PFF system (Fig. 2) that implements this novel concept at the CLIC Test Facility (CTF3) at CERN. CTF3 provides a 135 MeV electron beam bunched at 3 GHz frequency with a beam-pulse length of 1.2 μs and a pulse repetition rate of 0.8 Hz [2].

The incoming beam phase is measured in two upstream phase monitors (ϕ_1, ϕ_2). While the beam transits the

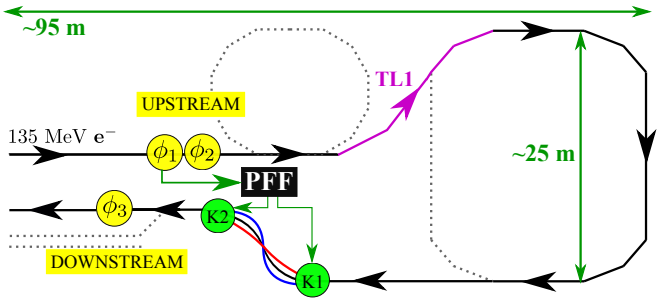

FIG. 2. Schematic of the CTF3 PFF prototype, showing the phase monitors (ϕ_1 , ϕ_2 and ϕ_3) and kickers (K1 and K2). The black box PFF represents the calculation and output of the correction. Bunches arriving early at ϕ_1 are deflected on to longer trajectories in the chicane (blue), and bunches arriving late on to shorter trajectories (red). Dashed lines indicate beam lines that are not used.

turnaround loop a phase-correction signal is evaluated and used to drive fast, high power amplifiers; these drive two electromagnetic kickers (K_1, K_2) which are used to alter the beam transit time in a four-bend chicane. A downstream phase monitor (ϕ_3) is used to measure the effect of the correction.

The beam time of flight between ϕ_1 and K_1 is around 380 ns. The total cable delay for the PFF correction signals is shorter, around 250 ns. The correction in the chicane can therefore be applied to the entirety of the beam pulse measured at the PFF input (ϕ_1), provided that the hardware latency is less than 130 ns. Significant hardware challenges include the resolution and bandwidth of the phase monitors, and the power, latency and bandwidth of the kicker amplifiers. A low latency digitiser/feedforward controller is also required.

The requirements of the CLIC system and their corresponding CTF3 values are listed in Table I. The main differences result from the different drive-beam energies. Higher power amplifiers (500 kW rather than 20 kW) are required for CLIC, which may be achieved by combining the output of multiple modules similar to those built for CTF3. CLIC also requires a distributed timing system to synchronise the phase of the drive and main beams along the 50 km facility, which is not addressed here.

The phase monitors [7] are cylindrical cavities with an aperture of 23 mm and a length of 19 cm. Small ridges (notch filters) in the cavity create an effective volume with a resonant frequency of 12 GHz. The resonant electromagnetic field induced by the beam traversing the cavity contains a beam-position-independent monopole mode and an unwanted position-dependent dipole mode. The effect of the latter is removed by summing the outputs from an opposing pair of feedthroughs, on the top and bottom of the cavity, via a RF hybrid. To extract the beam phase the output from each hybrid is mixed with a 12 GHz reference signal derived from a 3 GHz source which is phase-locked to the CTF3 RF system and serves

TABLE I. Requirements for the CLIC PFF system, and the respective CTF3 parameters; performance achieved with the prototype system is indicated by *****.

	CLIC	CTF3	
Drive beam energy	2400	135	MeV
No. PFF systems	50	1	
Kickers per PFF chicane	16	2	
Power of kicker amplifiers	500	**20***	kW
Angular deflection per kicker	±94	**±560***	μrad
Correction range	±10	**±6***	°
Correction bandwidth	> 17.5	$>$ **23***	MHz
Phase monitor resolution	< 0.14	**0.12***	°
Initial phase jitter	2.0	0.9	°
Corrected phase jitter	0.2	**0.2***	°

all three phase monitors. A linear response to input beam phase was measured over the range ±70° [8]. By comparing the signals from ϕ_1 and ϕ_2 we have measured a phase resolution of 0.12°, i.e. about 30 fs [9].

The phase signals are digitised in the feedforward controller board [9], which is used to calculate and output the amplifier drive signals, and to control the correction timing. It consists of nine 14-bit analogue to digital converters clocked at 357 MHz, a field programmable gate array, and four digital to analogue converters.

The kicker amplifiers [9] consist of one central control module and two drive and terminator modules (one per kicker). The control module distributes power and input signals to the drive modules. The 20 kW drive modules consist of low-voltage Si FETs driving high-voltage SiC FETs; an input voltage range of ±2 V corresponds to an output range of ±700 V. The response is linear to within 3% for input voltages between ±1.2 V, and the output bandwidth is 47 MHz for small signal variations of up to 20% of the maximum. For larger signal variations the bandwidth is slew-rate limited.

The two electromagnetic stripline kickers [10] are 1 m in length and have an internal aperture of 40 mm between two strips placed along their horizontal walls. They are designed to give a response within a few ns of the input signal. Opposite polarity voltages of up to 700 V applied to the strips at the downstream end horizontally deflects the 135 MeV beam by up to 560 μrad.

The measured total latency of the phase monitor signal processing, the feedforward calculation, and amplifier response was approximately 100 ns. Therefore the output from the controller was delayed by an additional 30 ns to synchronise the correction at the kicker with the beam arrival [9].

The PFF operation placed severe constraints on the setting of the magnetic lattice in both the beamline between the upstream phase monitors and the correction chicane, and in the chicane itself. The beam transfer matrix coefficient R_{52} between the two kickers characterises the change in path length through the chicane relative

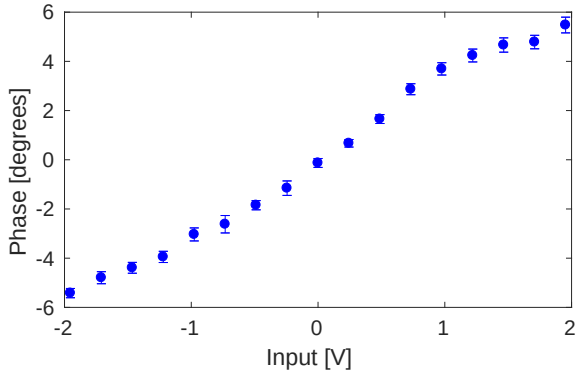

FIG. 3. Measured downstream beam phase vs. kicker amplifier input voltage. Standard errors are shown.

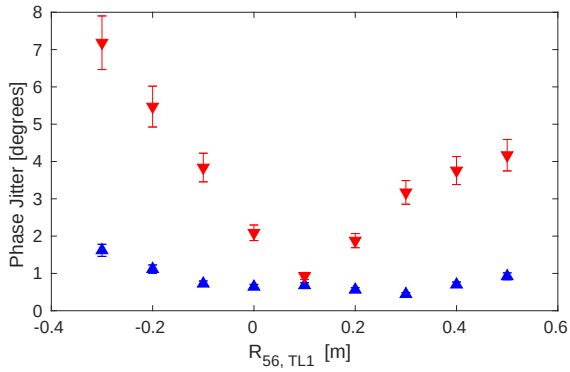

FIG. 4. Measured downstream (red) and upstream (blue) phase jitter vs. TL1 R_{56} value. Standard errors are shown.

to the deflection applied at the first kicker. With an R_{52} value of 0.74 m/rad [9] the expected maximum path length change for operation of the PFF system, corresponding to the maximum deflection of ± 560 μrad from each kicker, is about ± 400 μm, equivalent to $\pm 6^\circ$ in phase (Fig. 3). PFF operation also should not change the beam trajectory at the exit of the chicane. Therefore the chicane magnets were set so that the second kicker cancels the transverse orbit deviation created by the first [9].

A further challenge to PFF operation was obtaining a high correlation between the upstream and uncorrected downstream phases measured at ϕ_1 and ϕ_3 respectively. A correlation coefficient of at least 97% is required to reduce a typical incoming phase jitter of 0.8° to the target of 0.2° [9]. The maximum measurable correlation depends on both the phase monitor resolution and any additional phase jitter introduced in the beamlines between ϕ_1 and ϕ_3. The monitor resolution of 0.12° limits the maximum upstream-downstream phase correlation to 98% in typical conditions, and places a theoretical limit of 0.17° on the measurable corrected downstream phase jitter. The dominant beam source of uncorrelated downstream phase jitter arises from energy jitter that is transformed into phase jitter in the beamlines between ϕ_1 and ϕ_3.

To first order the phase dependence on energy can be described via the beam transfer matrix coefficient R_{56}: $\phi_3 = \phi_1 + R_{56}(\Delta p/p)$, where $\Delta p/p$ is the particle's relative energy error. The optimal condition is $R_{56} = 0$. This was achieved by tuning the R_{56} value in the 'TL1' transfer line (Fig. 2) so as to compensate for non-zero R_{56} in the other beamline sections. With $R_{56,\mathrm{TL1}} = 10$ cm the downstream phase jitter is reduced to the same level as the upstream jitter (Fig. 4). However, a large second-order phase dependence on energy remained uncorrected, resulting in a degradation in upstream-downstream phase correlation if there are drifts in beam energy.

The PFF system acts to remove the ϕ_1 phase, multiplied by a 'gain' factor, from the phase at ϕ_3. If the

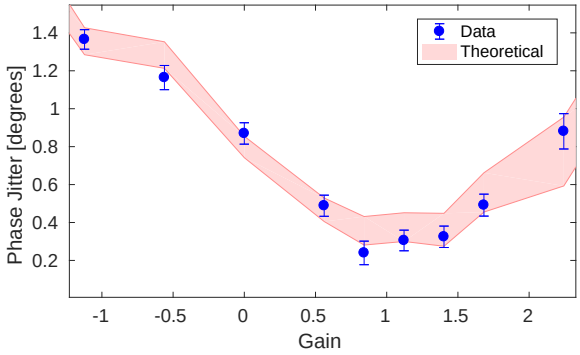

FIG. 5. Measured corrected beam phase jitter at ϕ_3 vs. PFF gain; standard errors are shown (points). The theoretically-achieveable performance is shown by the red shaded region (see text).

phases at ϕ_3 and ϕ_1 are fully correlated, and the jitters are identical, the optimal system gain is unity. In practice the gain is chosen to achieve optimal performance for real beam conditions. A representative gain scan is shown in Fig. 5. The optimal gain is typically in the range 0.9–1.3. Also shown in Fig. 5 is the theoretical prediction of the corrected phase jitter at ϕ_3, given the initial beam phase jitters at ϕ_1 and ϕ_3, the upstream-downstream phase correlation, and the gain. The simulation reproduces the data.

The PFF system simultaneously corrects pulse-to-pulse phase jitter and phase variations within the 1.2 μs beam pulse at CTF3. Fig. 6 shows the effect of the PFF system on the intra-pulse phase variations. The PFF system was operated in interleaved mode, with the correction applied to alternating pulses only. This allows the initial ('PFF Off') and corrected ('PFF On') downstream phase at ϕ_3 to be measured at the same time. The ϕ_1 (PFF input) phase is also shown for comparison.

It is an operational feature at CTF3 that there is a roughly parabolic phase sag of 40° along the pulse0,

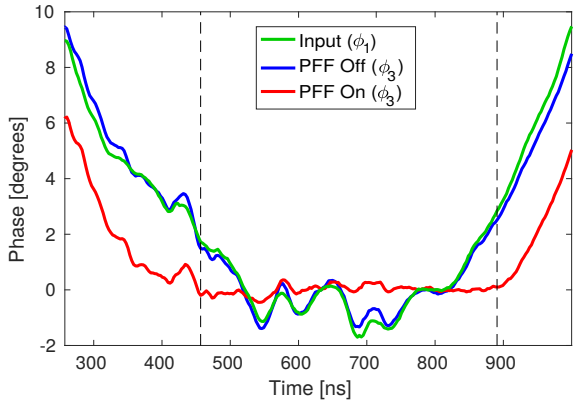

FIG. 6. Phase vs. time within the central portion of the beam pulse; the incoming phase measured in ϕ_1 (green), and the downstream phase measured in ϕ_3 with PFF off (blue) and PFF on (red). Each trace is the average over a 30 minute dataset. The vertical dashed lines mark the time interval corresponding to the PFF dynamic range.

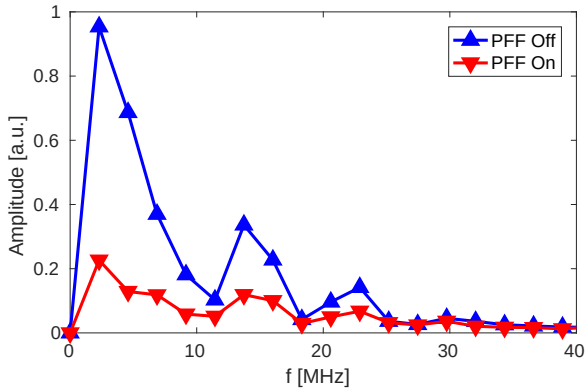

FIG. 7. Amplitude of phase errors at different frequencies (f) with the PFF system off (blue) and on (red).

resulting from the upstream RF pulse compression scheme [2]. Hence approximately a 440 ns portion of the pulse is within the $\pm 6°$ dynamic range of the PFF system, and can be corrected to zero nominal phase. This time duration for the full correction exceeds the CLIC drive-beam pulse length of 240ns and in any case the CLIC design avoids such a large phase sag [2]. Vertical dashed lines in Fig. 6 mark the 440 ns portion of the pulse where full correction is possible, and this range is used in the following analyses.

Within the range the PFF system flattens the phase, and almost all variations are removed. Residual offsets are still present where there are small uncorrelated differences between the initial phase at ϕ_1 and ϕ_3. The average intra-pulse phase variation (rms) over the dataset is reduced from $0.960 \pm 0.003°$ (PFF off), to $0.285 \pm 0.004°$ (PFF on).

In order to meet CLIC requirements (Table I) the PFF

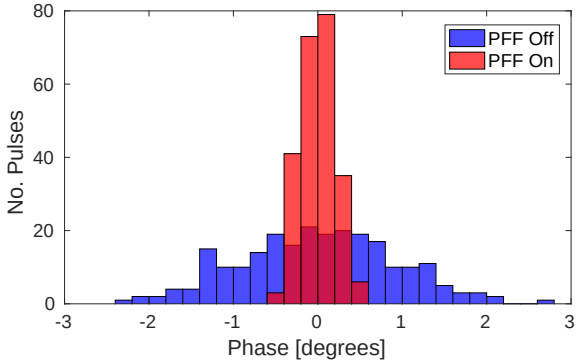

FIG. 8. Distribution of the mean downstream phase with the PFF system off (blue) and on (red).

correction bandwidth should be at least 17.5 MHz. A Fourier-Transform (FFT) method was used to characterise the PFF on/off datasets. The FFT amplitude is shown vs. frequency in Fig. 7. It can be seen that phase errors are corrected by up to a factor of 5 for frequencies up to 23 MHz, above which they are smaller than the monitor resolution and not measurable. This is consistent with an expected system bandwidth of around 30 MHz, and exceeds the CLIC requirement.

The effect of the PFF system on the pulse-to-pulse jitter, i.e. the jitter on the mean phase of each beam pulse, is shown in Fig 8 for a dataset of around ten minutes duration. The pulse-to-pulse phase jitter is reduced from $0.92 \pm 0.04°$ to $0.20 \pm 0.01°$, meeting CLIC-level phase stability. The system acts to remove all correlation between the upstream and downstream phase, reducing an initial correlation of $96 \pm 2\%$ to $0 \pm 7\%$ for this dataset. Given the incoming upstream phase jitter and measured upstream-downstream correlation, the performance is consistent with the theoretically predicted correction of $0.26 \pm 0.06°$.

Typically this level of corrected phase stability could not be maintained for longer time periods due to drifts in the CTF3 RF system, which led to a degradation in the upstream-downstream phase correlation as well as mean phase drifts beyond the PFF correction range. Nevertheless a mean phase stability of 0.30° was achieved in datasets taken over periods as long as 20 minutes. With suitable upstream RF feedbacks to keep the beam phase within the correction range, and a reduction of the higher order phase-energy dependence in the magnetic lattice, the system is capable of achieving CLIC-level phase stability continuously.

The system was further tested by varying the incoming mean beam phase systematically by around $\pm 3°$ (Fig. 9). Variations of this magnitude are comparable to the expected conditions in the CLIC design (Table I). This is illustrated in Fig. 9. The system removed the induced phase variations and achieved more than a

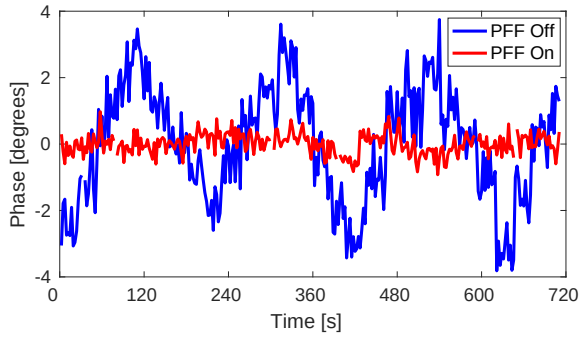

FIG. 9. Mean downstream phase vs. time with the PFF system off (blue) and on (red) subject to large additional phase variations added to the incoming phase (see text).

factor-5 reduction in the downstream phase jitter, correcting from $1.71 \pm 0.07°$ to $0.32 \pm 0.01°$.

In summary, we have built, deployed and tested a prototype drive-beam phase feedforward system for CLIC. The system incorporates purpose-built high-resolution phase monitors, an advanced signal-processor and feedforward controller, low-latency, high-power, high-bandwidth amplifiers, and electromagnetic stripline kickers. The phase-monitor resolution was measured to be $0.12° \simeq 30$ fs. The overall system latency, including the hardware and signal transit times, was measured to be approx. 350 ns, which is less than the beam time of flight between the input phase monitor and the correction chicane. The system was used to stabilise the pulse-to-pulse phase jitter to $0.20 \pm 0.01° \simeq 50$ fs, and to simultaneously correct intra-pulse phase variations at frequencies up to 23 MHz.

This technique offers an additional application for stabilising the electron-beam arrival at FELs, where 'pump-probe' experiments require laser/electron synchronisation ideally to the few femtosecond level, see e.g. [11]. The current state-of-the-art in synchronisation at FELs is approx. 30 fs, using all-optical techniques [12].

Our results are limited to a similar precision by the beam arrival-time monitor resolution of $\simeq 30$ fs, which was designed to meet the CLIC requirements. In [5] a device was described, based on an electro-optic bunch monitor, which was able to measure an electron-bunch arrival time to approx. 6 fs. If such a device were used to provide an input to a feed-forward system as described here there would be the possibility of stabilising the beam arrival time to better than 10 fs, which would represent a significant advance towards the desired femtosecond level. A key feature of our system is that it incorporates a beam turnaround, which provides sufficient beam delay to allow a feed-forward correction to be derived and applied. FELs based on energy-recovery linacs (ERLs) (see e.g. [13–15]) intrinsically incorporate a beam turnaround section that would enable the deployment of a system based on our technique.

In conclusion, given our demonstration of a high-precision feed-forward system, beam-arrival monitors with improved temporal resolution, and ERL-based FEL designs, a next-generation FEL facility with femtosecond-level synchronisation capability seems feasible.

We acknowledge Alessandro Zolla and Giancarlo Sensolini (INFN Frascati) for the mechanical design of the phase monitors and kickers, and Alexandra Andersson, Luca Timeo and Stephane Rey (CERN) for their support on the phase monitor electronics. We thank the operations team of CTF3 for their outstanding support. This work was supported by the the UK Science and Technology Facilities Council, and by the European Commission under the FP7 Research Infrastructures project EuCARD, grant agreement no. 227579.

[1] CLIC and CLICdp collaborations, "Updated baseline for a staged compact linear collider," CERN-2016-004 (2016).
[2] M. Aicheler *et al.*, "CLIC conceptual design report," CERN-2012-007 (2012).
[3] H. Abramowicz *et al.*, Eur. Phys. J. C (Submitted), CLICdp-Pub-2016-001 (2016).
[4] D. Schulte and R. Tomas, in *Proceedings of PAC09* (Vancouver, Canada, 2009) pp. 3811–3813.
[5] F. Löhl *et al.*, Phys. Rev. Let. **104**, 144801 (2010).
[6] A. Gerbershagen *et al.*, Phys. Rev. AB **18**, 041003 (2015).
[7] F. Marcellini *et al.*, EuCARD-REP-2013-023 (2014).
[8] P. Skowronski *et al.*, in *Proceedings of IPAC13* (Shanghai, China, 2013) pp. 2097–2099.
[9] J. Roberts, DPhil thesis, University of Oxford (2016).
[10] A. Ghigo *et al.*, in *Proceedings of IPAC2011* (San Sebastian, Spain, 2011) pp. 1000–1002.
[11] E. Savelyev *et al.*, New. J. Phys **19**, 043009 (2017).
[12] S. Schulz *et al.*, Nat. Commun. **6**, 5938 (2015).
[13] J. Sekutowicz *et al.*, Phys. Rev. STAB **8**, 010701 (2005).
[14] K. Kim *et al.*, Phys. Rev. Let. **100**, 244802 (2008).
[15] F. Jackson *et al.*, Phys. Rev. AB **19**, 120701 (2016).